

## Variation of the Chemistry of the Dead Sea Brine as Consequence of the Decreasing Water Level

Jamal Abu-Qubu<sup>1</sup> · Broder Merkel<sup>2</sup> · Volkmar Dungel<sup>2</sup> · Omar Rimawi<sup>3</sup>

Received: 4 November 2017 / Accepted: 13 March 2018 / Published online: 15 March 2018  
© Springer Science+Business Media B.V., part of Springer Nature 2018

**Abstract** For many years, the Dead Sea suffers from an annual inflow deficiency of about one billion cubic meters, flood and baseflow. The water level changes are related to the majority of surface water inflows diverted for irrigation purposes, in addition to intensive loss of water by the high rate of evaporation and industrial water use. This causes the Dead Sea water level to decline about 35 m within the last 50 years for a long-term average of about 0.79 m per year. The changes in the hydrochemical composition were simulated experimentally to determine the changes that take place as a function of brine water evaporation level and its density. The Total Dissolved Solids (TDS) and the density of the Dead Sea water varies as a function of its water evaporation level changes. It was found that the density variation is not following a linear function with respect to water volume changes. But it follows the total amount of precipitate that occurred at different water levels. The electrical conductivity (EC) changes with respect to time and the prevailing temperature. There was no formula to calculate the high salinity of brine water above the normal ocean water. Consequently, the EC measurements were adopted to represent the Dead Sea water salinity. But in this research a converging factor (0.80971) has been found to convert the TDS values into salinity values. On contrary, the pH values revealed an inverse relationship with respect to the evaporation levels.

---

✉ Jamal Abu-Qubu  
qubu.jamal@gmail.com

Broder Merkel  
merkel@geo.tu-freiberg.de

Volkmar Dungel  
dungerv@geo.tu-freiberg.de

Omar Rimawi  
rimawiom@ju.edu.jo

<sup>1</sup> Ministry of Energy and Mineral Resources, Amman, Jordan

<sup>2</sup> TU Bergakademie Freiberg, Freiberg, Germany

<sup>3</sup> The University of Jordan, Amman, Jordan

**Keywords** Density · Precipitation · Halite · Bischofite · Sylvite · Tachyhydrite · Carnallite

## 1 Introduction

The total runoff of the northern catchment entering to the Dead Sea revealed a continuous reduction due to the increasing water diversions. The severe reduction started since early 1960s, when the highest inflow was recorded with  $2125 \times 10^6 \text{ m}^3$  in 1968/1969. On contrary, the lowest inflow through the Jordan River since the 1960s was recorded with  $282 \times 10^6 \text{ m}^3$  in 1990/1991. Surface water reaching the Dead Sea through the Jordan River Valley (JRV) includes irrigation return flow, which has been estimated to be about 15% of the total inflow (Margane et al. 2002; Ministry of Water and Irrigation 2013). According to the yearly storage records of the Water Authority of Jordan (WAJ), about 105 million cubic meters of runoff and baseflow are captured by side-wadi reservoirs, while the total capacity of the artificial reservoirs is 450 million cubic meters (Margane et al. 2002). Some of these dams partly recharge the aquifer in the area and feed some perennial springs close to the Dead Sea shoreline.

The groundwater table in the aquifers adjacent to the Dead Sea has declined in the last decades due to pumping rates that exceeded the safe yield. Therefore, water tables dropped and many springs in the side-wadis discharging into the Dead Sea Basin dried up. Other water withdrawals in the West Bank and Wadi Araba are assumed to be taken mainly from deep groundwater and thus do not affect the surface water balance (TAHAL Group 2011).

By the early 1980s, the Dead Sea water has reached the point that Halite ( $\text{NaCl}$ ) started to precipitate (Steinhorn and Gat 1983). Gypsum apparently continues to precipitate in the Dead Sea at small quantities, but it is obscured by the higher quantities of halite precipitation (Herut et al. 1998). A proportionally smaller decrease in comparison to  $\text{Na}^+$  was observed for  $\text{Cl}^-$  (Gavrieli 1997).

Assuming that the Dead Sea will continue to receive extremely reduced inflow and will lose water by evaporation and industrial uses, the surface water level will drop further in the range between 0.79 measured in 2015/2016 and 1 m/year as an average decline within the last decade (Arab Potash Company Annual Reports 1993). Consequently, the chemical characteristics of the Dead Sea water will be changed at different evaporation levels as well.

During the evolution of the Dead Sea water level changes, the chemical composition of the brine changes due to precipitation of different types of salts. If, e.g., gypsum is precipitated consequently, part of the sulfate is removed from the subsurface brine.

Considerable gypsum precipitation occurred in the Dead Sea waters during the late 1950s until early 1960s (Neev and Emery 1967). The precipitation of gypsum in the late 1950s is assumed to happen during periods of deficit water balance. Significant gypsum precipitation occurred in the Late Pleistocene Lake Lisan (Stein et al. 1997). However, by the early 1980s, gypsum deposition rates were three times less, compared with the rates recorded in the 1950s. Precipitation of gypsum was recognized in sampled sediments from the center of the lake in the middle of nineteenth century as well as in the 1970s (Beyth 1980). The reduction in the gypsum accumulation rate is in accordance with the declining  $\text{SO}_4/\text{Ca}$  ratio (Reznik et al. 2009).

To investigate the changes of the brine composition in the wake of evaporation and consequent precipitation of minerals, several experiments were conducted in the laboratory to

simulate the future reduction of the Dead Sea water level, contemporaneously with water EC, TDS and density changes.

## 2 Methodology

### 2.1 Experiment 1

Experiments were carried out to simulate the EC of the Dead Sea water prior to 2016. Experiments were performed, by adding a specified amount of distilled water corresponding to the percentage of the evaporated amount, relative to the water volume available in the Dead Sea Basin. Thereto, the present water column of the Dead Sea water was considered to be around 300 m and the average annual drop in the water height of the Dead Sea was assumed to be 1 or 10 m in 10 years, respectively. The ratio between the water head loss during 10 years (10 m) and the actual water height (300 m) was then 1:30. Consequently, 50 ml of distilled water was added to 1500 ml of the Dead Sea water to simulate a 10 years period in the past. In order to simulate the previous situation of water salinity of the Dead Sea, salt sampled from the Dead Sea were added to the mixed water to recover the previous status before the first 10 years interval. The add salt was completely dissolved to reach the saturation level. Then, the brine of each 10 years interval was heated up to 40 °C representing the average summer temperature in the area. During the heating, the electric conductivity (EC) and the pH values were measured at temperatures of 15, 20, 25, 30, 35, and 40 °C, respectively, using WTW-device (InoLab Cond Level 1). This was repeated five times.

### 2.2 Experiment 2

The densities were measured for each 10-year interval by using the Pycnometer tool (Rice et al. 2017). The method depends on weighing the empty flask (Pycnometer), and then, it was weighed again filled with 50 ml of the brine. Consequently, the difference is the weight of the brine. The obtained weight of the brine is then divided by fifty to get the density of the brine measured in g/L. Parallel to these experiments, another procedure was used to obtain the TDS in the brine. The experiments were conducted according to the standard methods for the examination of water and wastewater, (Greenberg et al. 1980), by filling a 250-ml beaker with 100 ml of the brine water, thereafter, it was dried in an oven at 104 °C overnight (about 15 h), and the weight of the remained solids were weighed on a four digit sensitive balance (BOECO). Next stage, the dried-up salts were again returned to the oven and heated at 180 °C overnight (Greenberg et al. 1980), and finally, the dried-up solids were weighted. It is noted that the salts are not completely dried up; this indicates that the APHA standard is not applicable in the case of the Dead Sea brine water. Therefore, the salts returned again to the oven for 3 h at 300 °C (by trial and error) until the salts weight is constant. Thereafter, the TDS is measured for each time interval by multiplying the gained weight of dried solids by 10 to get the TDS in 1 L of brine water.

### 2.3 Experiment 3

In addition, laboratory experiments were performed, to investigate which minerals will be formed at certain stages of brine enrichment. As for the other experiments, brine was sampled

from the upper most part of the Dead Sea basin, because it is more likely that the upper strata of the Dead Sea will be impacted by evaporation and not the entire water column. The precipitated salts and the remaining water at each stage were investigated using different techniques. The experiments were conducted by using glass beakers with a volume of 2.5 L each. Then, the beaker filled with the Dead Sea brine and heated gradually to a temperature ranging between 60 and 80 °C, whereas the time needed for this stage is 6 h. Brine samples and samples of precipitated minerals were taken at different stages of evaporation. The precipitates are related to the evaporation level, which correspond to the gradual increase in temperature. This is a suitable simulation of the precipitates occur in the Dead Sea basin. Subsequent, the analyses conducted using the ICP-MS (Quantima, GBC Scientific Equipment) and the Bruker-X-ray Diffraction D4 Endeavour (XRD) device was used together with the software ICDD's search indexing programs, Sieve for PDF-2 designed to search and identify unknown materials. Sieve is integrated into the ICDD databases to allow the use of the extensive data mining.

Sampling of brine for the determination of major cations was performed at evaporating levels of 12.5, 20, 25, 37.5, 40 and 60%, respectively. The evaporation percentages were reached by direct heating in parallel experiments. Evaporation process was stopped at the 60% level, as far as the remaining water was captured between the salt crystals and cannot be liberated at temperatures less than the boiling point.

The density of the Dead Sea brine was determined by weighing a certain volume of brine (e.g. 10 cc) at 25 °C and calculating the density by dividing the weight by the volume. The EC was read in mS/cm with the EC-meter, whereby the option “automatic recalculation to 25 °C” was disabled.

The brine samples in the laboratory experiments were diluted 1:200 ml to achieve proper concentrations for the ICP-MS used to determine the concentration of major cations and trace elements. The X-Ray Fluorescence Spectrometer (XRF) was utilized for quantitative analysis of major elements percentages as well trace elements with concentrations below 200 ppm in solid samples.

### 3 Results and Discussion

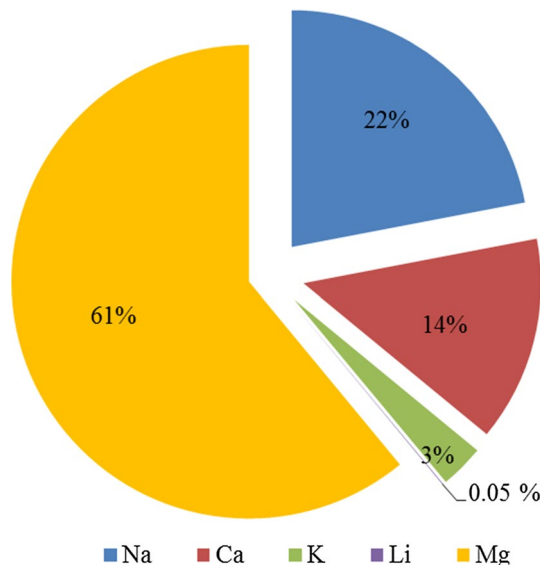
The tested original Dead Sea brine water contained about 340 g/L total dissolved salts and had a density of 1.241 kg/L which is compatible with (Ben-Yaakov and Sass 1977). This brine is rather unique with 99% Cl<sup>-</sup> and 1% Br<sup>-</sup> (molar concentration) as the most dominant anions. SO<sub>4</sub><sup>2-</sup> and inorganic C do not play an important role. Distribution of the cations in the Dead Sea brine is shown in (Fig. 1) with Mg<sup>2+</sup> being the most dominant cation.

These results deal with the end state waters entering the Dead Sea; that is the water in the basin of the Dead Sea, also including the returned waters from industrial works, which represent about 45% of the pumped waters. In addition, these waters represent the mixing of basin waters with all other possible sources, which are the stream waters including the surrounding spring waters and the possible deep aquifer waters in contact (interface) with the southern part of the Dead Sea and the rainfall waters, which interacts with the different rock types along their path to the basin.

#### 3.1 Experiments 1 and 2

The results shown in Table 1 represent the measured TDS and density values of the successive 10 years interval, started from 1956 until 2056. In addition, the calculated

**Fig. 1** Distribution of major cations in the Dead Sea brine (relative molar equivalents)



salinity values obtained by using the converting factor equal to (0.80971), which has been found in this research. It is clear that, the density values were decreasing since 1960s until 1986, but it was increasing thereafter continuously. The correlation between the measured densities by the Pycnometer equipment and the calculated densities for each 10-year interval revealed a consistency, where the measured densities showed slightly higher values than the calculated ones (Fig. 2). The correlation between any two relevant readings of the Pycnometer and the calculated shows that error is less than 5%, which can be attributed to acceptable personal errors.

**Table 1** The measured EC at 20 °C, TDS, calculated density, measured density and calculated Salinity of the Dead Sea brine water each 10 years interval

Year	EC (mS/cm)	TDS (g/L)	Calculated density	Pycnometer density	Salinity (g/kg)
2056	151.3	359	1.247	1.252	291.022
2046	160.2	359	1.245	1.251	290.310
2036	161.1	354	1.244	1.247	286.488
2026	167	348	1.242	1.245	281.662
2016	170.7	339	1.242	1.244	274.407
2006	174.1	331	1.242	1.243	268.318
1996	174.2	316	1.241	1.242	256.173
1986	174.4	305	1.240	1.241	246.975
1976	174.6	303	1.240	1.244	245.533
1966	175.4	292	1.242	1.244	236.044
1956	175.7	276	1.243	1.245	223.785

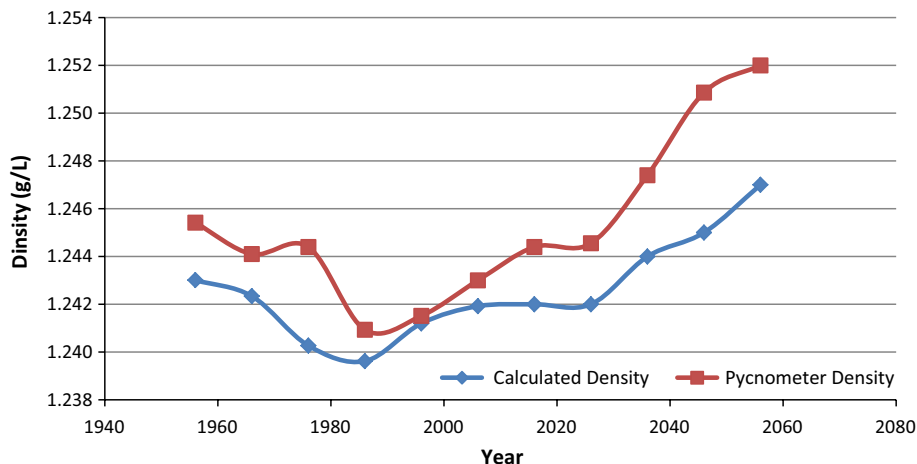


**Fig. 2** The calculated and the measured densities of the Dead Sea water each 10 years interval

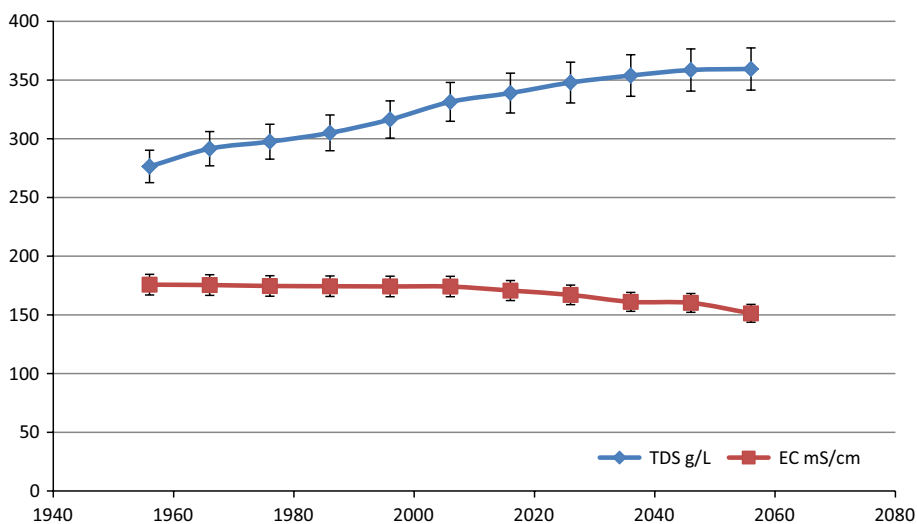


**Fig. 3** The Dead Sea water EC (mS/cm) compared with the TDS (g/L) each 10 years interval, Error bar is added for 5% value

The TDS values are slightly increasing with respect to evaporation level (10 years interval). On the other hand, the EC values converge down in a very slight decreasing trend, (Fig. 3). This is attributed to decreasing in the activity coefficients of the divalent ions by increasing the salinity and evaporation levels.

The TDS values also revealed no consistency with respect to the density values (Fig. 4). This is due to increasing TDS values, while the density changed from decreasing manner to increasing trend after 2016.

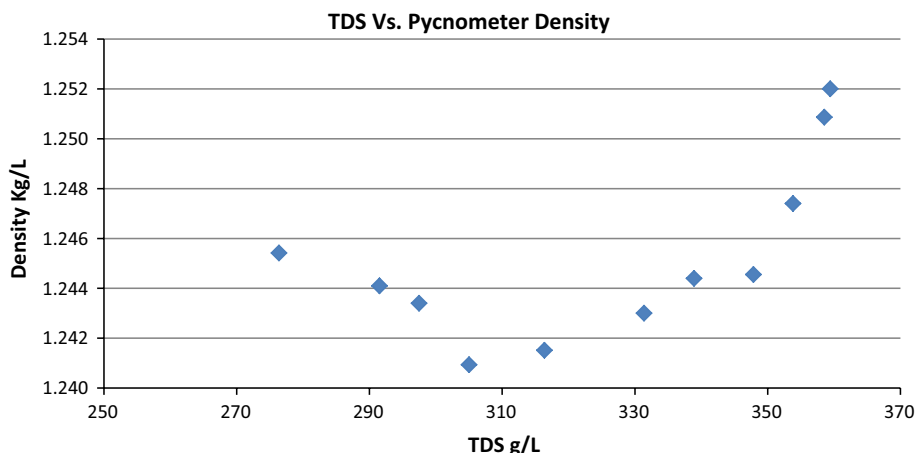


**Fig. 4** The Dead Sea water density relation with the TDS (10 years intervals)

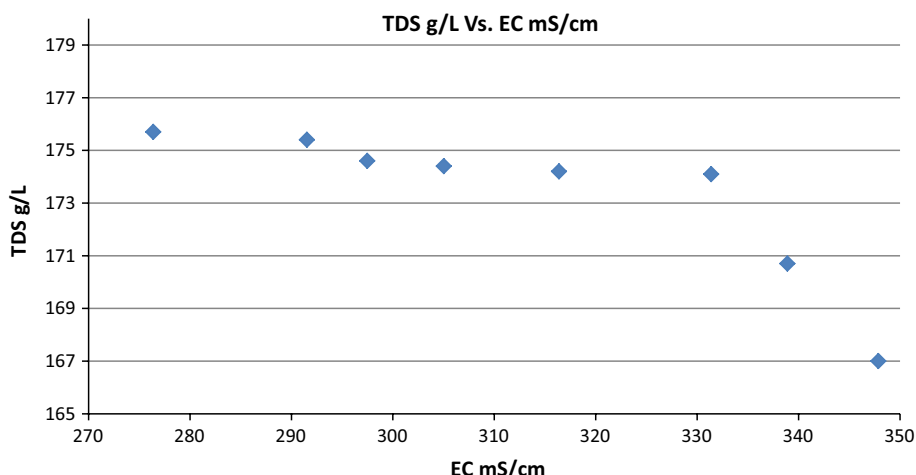


**Fig. 5** Measured TDS versus EC of the Dead Sea Brine

The conducted results from the different Dead Sea evaporation levels TDS versus EC (Fig. 5) are compatible with the Calibration Curve of the Salinity versus electrical conductivity (Fig. 6).

The pH value measured for different evaporation levels is shown in Table 2. The results in Fig. 7 indicate that the pH values are decreasing with respect to time that is the pH decreases as the evaporation is continued.

EC readings as function of time (1956–2056) and temperatures (15–40 °C) are presented in Table 3 and Fig. 8. These results achieved from the different experimental works on EC changes, revealed that the EC is decreasing proportionally with respect to different temperatures and decreases, as far as, evaporation continues year by year.

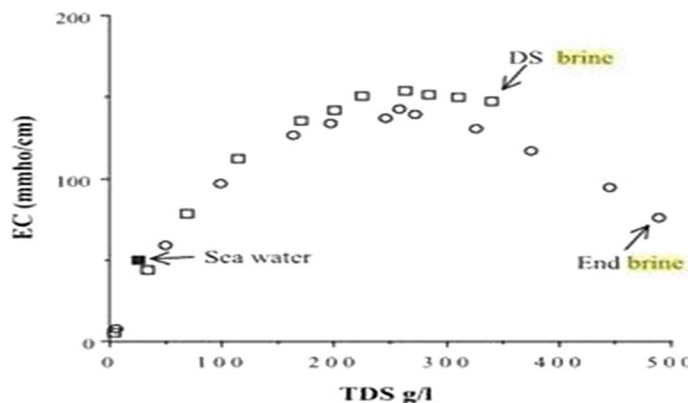


**Fig. 6** Calibration curve (salinity vs. electrical conductivity)

**Table 2** The pH values of the brine at different evaporation levels

Year	pH					
2056	5.69	5.7	5.76	5.81	5.82	5.83
2046	5.78	5.85	5.97	5.93	6.00	5.98
2036	5.80	5.86	5.89	5.95	6.02	6.07
2026	5.80	5.96	6.00	6.04	6.08	6.16
2016	5.91	5.94	5.99	6.08	6.10	6.17
2006	5.99	6.04	6.08	6.16	6.21	6.25
1996	6.00	6.04	6.09	6.16	6.21	6.25
1986	6.01	6.06	6.11	6.16	6.22	6.26
1976	6.02	6.06	6.11	6.17	6.23	6.27
1966	6.04	6.07	6.13	6.18	6.23	6.27
1956	6.06	6.07	6.13	6.21	6.25	6.28

It is obvious that the EC changes as a function of time (on annual bases), at a specific temperature are relatively small. EC changes in the Dead Sea brine can be noticed, clearly, every 10 years. In the 10 years increments, small variations can be attributed to the precipitation of some salts. EC drops when the temperature decreased from 40 to 30 °C, but less over the range from 25 to 15 °C. The increase in the TDS is attributed in this specific case due to the precipitation of monovalent and partially divalent salts, while the decrease in the EC is attributed to the dominancy of calcium and magnesium ions (divalent ions with low ionic activities) and chloride ions content. The calcium chloride is highly soluble salt and normally will stay in solution (Fig. 8).

### 3.2 Experiment 3

The results achieved from ICP-MS analyses of the remained Dead Sea water at different evaporation levels displayed that the hydrochemical characteristics—chemical and mineralogical composition—were changed successively. The cations in the residual water, Mg and Ca are increasing as the evaporation advanced, while the Na and K are decreasing with increasing evaporation levels, Table 4 and Fig. 9.

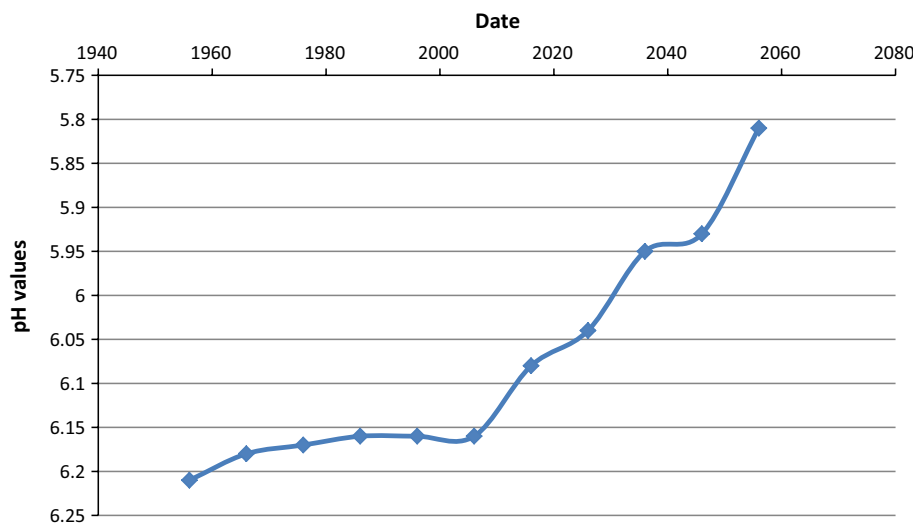


**Fig. 7** The decreasing pH values with respect to evaporation level

**Table 3** The EC (mS/cm) changes of the Dead Sea water at different temperatures

Year	Temperature (°C)					
	40	35	30	25	20	15
2056	161.1	158.2	152.2	151.7	151.3	149.8
2046	173.1	172.5	170.1	162.1	160.2	156.5
2036	174.5	174.1	170.5	162.8	161.1	158.2
2026	174.6	174.3	171.9	167.8	167	165
2016	176.6	175.9	173.5	171.9	170.7	170.3
2006	179.7	179.5	176.7	175.5	174.1	173.5
1996	180	179.5	177.2	175.7	174.2	173.8
1986	180	179.6	177.5	175.7	174.4	174.1
1976	181	179.8	177.8	175.8	174.6	174.3
1966	181.8	179.9	178	176.2	175.4	174.9
1956	181.8	179.9	178.4	177.1	175.7	175.1

The main components of the residual water at different evaporation levels are  $\text{Na}^+$ ,  $\text{Ca}^{2+}$ ,  $\text{K}^+$ ,  $\text{Mg}^{2+}$ , and  $\text{Cl}^-$ . It is clearly indicated from Table 4 that  $\text{Na}^+$  decrease continuously and  $\text{K}^+$  decreases after the first evaporation level, on contrary to an increase in  $\text{Mg}^{2+}$  and  $\text{Ca}^{2+}$  concentrations. The variations in  $\text{Na}^+$ ,  $\text{K}^+$ ,  $\text{Ca}^{2+}$  and  $\text{Mg}^{2+}$  ions concentrations are attributed to the type of the minerals precipitated at the different evaporation levels as represented in Tables 5 and 6.

The XRD analyses of the precipitate indicate the presence of Halite and Sylvite at the 12.5% evaporation level. This phenomenon explained the decrease in the  $\text{Na}^+$  and  $\text{K}^+$  all over the following evaporation levels. But sylvite is only precipitated at the initial stages and in the later stages K-ions precipitated as ion substitute in the other minerals

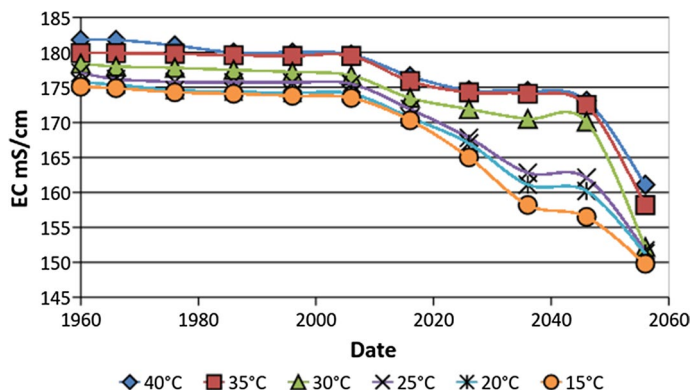


**Fig. 8** Changes of electric conductivity (EC) over time at different temperatures

**Table 4** The ICP-MS analyses of the remained Dead Sea water at different evaporation levels

Evaporation level %	Density (g/L)	Na (ppm)	Ca (ppm)	K (ppm)	Mg (ppm)
0	1.241	27,900	19,500	8300	52,700
12.5	1.277	11,930	22,050	11,060	61,430
20	1.242	10,470	23,810	10,430	64,270
25	1.194	5965	25,910	10,360	70,970
37.5	1.301	2591	32,390	2702	82,880
40	1.284	1811	32,460	1607	92,430
60	1.195	1581	61,650	1094	96,510

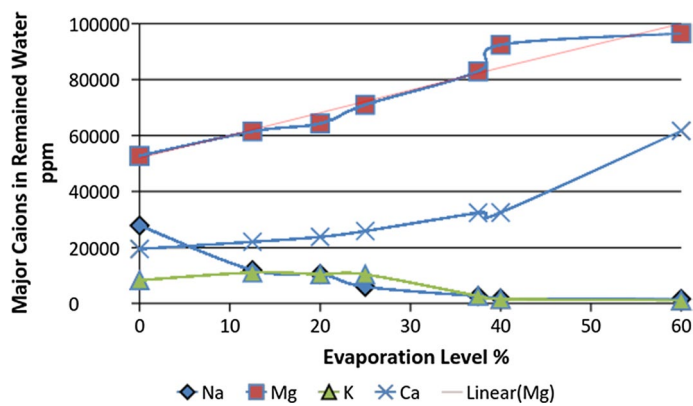


**Fig. 9** Comparison of different cations in the remained water at different evaporation levels

precipitated at different evaporation levels. The other mineralogical constituents of the precipitates are Bischofite ( $\text{MgCl}_2 \cdot 6(\text{H}_2\text{O})$ ), Tachyhydrite ( $\text{CaMg}_2\text{Cl}_6 \cdot 12(\text{H}_2\text{O})$ ) and Carnallite ( $\text{KMgCl}_3 \cdot 6(\text{H}_2\text{O})$ ). In the industrial process of brine evaporation, Halite

**Table 5** XRF results of precipitates at different evaporation levels

Evaporation level (%)	Na wt%	Mg wt%	K wt%	Cl wt%	Br wt%	Ca wt%	Si wt%	P wt%	Fe wt%	Mn wt%
12.5	17.60	5.96	3.22	57.00	2.96	9.78	0.20	0.02	0.10	0.010
25.0	15.10	9.63	5.68	57.40	2.14	6.24	0.13	0.01	0.09	0.012
37.5	14.00	11.00	7.98	54.70	1.78	6.10	0.09	0.01	0.09	0.020
50.0	21.90	9.01	3.05	55.50	1.73	4.39	0.14	0.03	0.10	0.021
62.5	17.10	11.30	3.13	55.30	1.92	6.20	0.12	0.03	0.16	0.035
75.0	8.16	14.10	4.93	57.90	2.94	7.71	0.06	0.02	0.17	0.021
100	2.15	16.80	4.93	58.00	4.35	9.46	0.07	0.11	0.17	0.025
Float > 30	2.72	17.20	3.96	58.10	3.16	9.80	0.07	0.02	0.10	0.015

**Table 6** XRD analyses of the Dead Sea water precipitates at different evaporation levels

Evaporation level (%)	Halite <sup>a</sup>	Bischofite	Sylvite	Tachyhydrite	Carnallite
12.5	**** <sup>b</sup>	**	**	—	—
25	****	**	*	—	***
37.5	****	**	*	**	***
50	****	**	*	**	**
62.5	****	**	*	**	**
75	****	***	*	***	**
100	***	****	*	***	**
> 30	***	****	*	***	**

Key based on relative XRD high peak data

<sup>a</sup>Halite NaCl, Bischofite MgCl<sub>2</sub>·6H<sub>2</sub>O, Sylvite KCl, Tachyhydrite CaMg<sub>2</sub>Cl<sub>6</sub>·12H<sub>2</sub>O, Carnallite KMgCl<sub>3</sub>·6(H<sub>2</sub>O)

<sup>b</sup>Major \*\*\*\*, Intermediate \*\*\*, Minor \*\*, Trace \*, Not detected –

precipitates and at a density of about 1.3 kg/L, and also Carnallite begins to precipitate. In the factories, the latter is dissolved and potash is produced (TAHAL Group 2011). The Dead Sea water at present is supersaturated with respect to several minerals including Gypsum, Anhydrite, Barite, Celestite and Halite. Among these minerals, only Halite precipitated in the Dead Sea in large amounts, while Gypsum is assumed to precipitate at a very slow rate (Reznik et al. 2009). The evaporation in the laboratory experiment was continued to advanced levels. Then, a floated thin layer was formed at the surface of the water. Thus, this floating layer makes a barrier that after certain thickening stalactites started to form (Fig. 10a). This can be observed in natural deposits, where the regression of the Dead Sea shorelines were occurred (Fig. 10b).

During the evaporation level of 37.5%, a thin film of a precipitate occurred at the surface of the water. This floated film remained at the surface until it reached the evaporation level of 62.5%. This means that the water at 37.5% evaporation level has a density capable to carry the formed precipitate. By further evaporation levels, the sodium content is sharply decreased until the end of the experiment (Tables 4, 5, 6 and Figs. 9, 11). The Mg<sup>2+</sup> and K<sup>+</sup> constituents of the Dead Sea water are observed to follow the same trend as

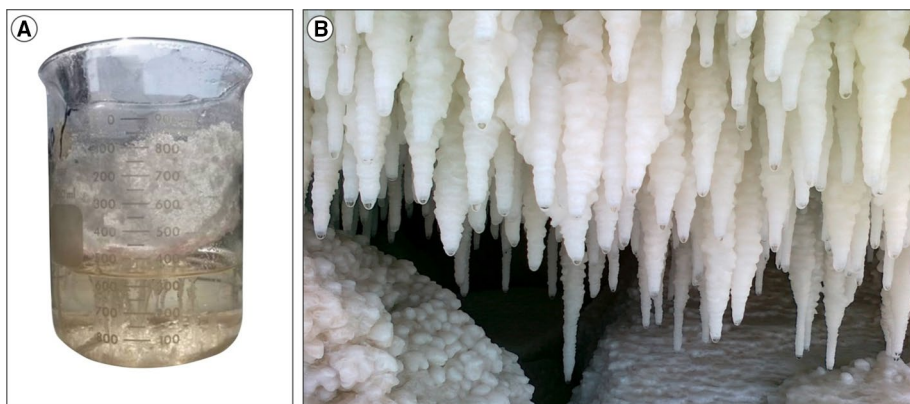


**Fig. 10** **a** Stalactites formed in laboratory experiment, **b** Stalactites along the Dead Sea shoreline (Photo courtesy of Khaled Moumani)

indicated in Fig. 11. In general, up to 37.5% evaporated water level, both Na and Ca ions are found to decrease at this stage and further stages. Even with the reduction of Ca content, no gypsum is precipitated; hence, no turbidity occurred and consequently no “Whitening” phenomenon is observed.

The “Whitening” phenomenon was observed in August to December of the year 1943; when 18 mg/L of solid material was found and 80% of the solid material consisted of calcium carbonate (Bloch et al. 1944). The same phenomenon was observed in August 1959, when a decrease in transparency from the common value of 3 m to values lower than 1 m was observed (Neev and Emery 1967).

On the other hand, the  $K^+$  content started to decrease continuously after the 37.5% evaporation level, which means that K-minerals was precipitated at this stage. In general, the 37.5% evaporation level is considered to be the critical overturning point of the Dead Sea water at which recognizable changes of the hydrochemical characteristics of the Dead Sea water are occurring. It is important to mention that nature does not follow the laboratory experiments. Therefore, the conducted experiments over the coming 50 years patch time in

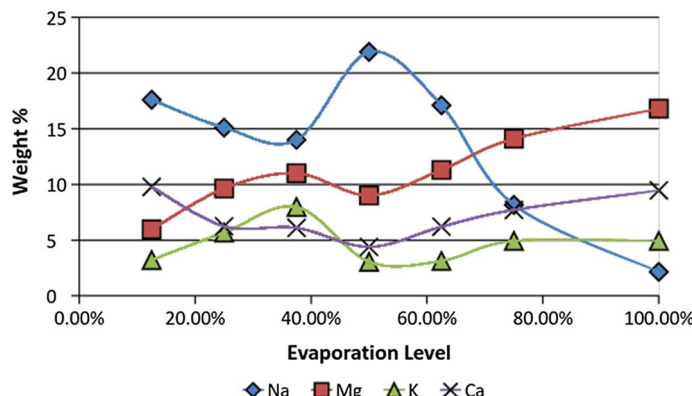


**Fig. 11** Comparison of different cations in precipitated salts at different evaporation levels

this research does not duplicate the exact condition of the Dead Sea, where many parameters are involved in natural conditions but are excluded to simplify the experimental works.

The correlation matrix between the different analyzed constituents of the precipitate at different evaporation levels (Table 5) is presented in Table 7. On the other hand, the related P-Values are presented in Table 8. It is obviously noted that the positive relationships are less dominant in comparison with the negative relationships. This is an indication that the proportional relation between different elements is dominated in this case study. The correlation coefficient between Na and Mg was ( $r=-0.881$ ,  $P=0.00385$ ). The same negative correlation coefficient ( $r=-0.898$ ,  $P=0.00244$ ) was obtained between Mg and Si. This negative correlation indicates an inverse relation. The positive correlation was found between Ca and Br ( $r=0.92857$ ,  $P=0.00086$ ), Cl with Br ( $r=0.83333$ ,  $P=0.01018$ ), Cl with Ca ( $r=0.7857$ ,  $P=0.02082$ ), Na with Si ( $r=0.87427$ ,  $P=0.00451$ ) P with Fe ( $r=0.75641$ ,  $P=0.02985$ ) and lastly P with Mn ( $r=0.71463$ ,  $P=0.04637$ ). This group of elements showed the proportional relation that is each correlated two elements either increasing or decreasing together.

The relationships between the different major constituents can only be explained by interpreting the different solids or precipitates at different evaporation levels, whereas Na minerals as Halite and Mg minerals such as Bischofite, Tachyhydrite and Carnallite are started to precipitate or stopped from precipitation contemporaneously.

## 4 Conclusions

The conducted experiments in this research showed that the TDS values for the Dead Sea hypersaline waters can be converted into salinity values using the empirical number (0.80971). The TDS values and the density values are not correlated to each other, neither by proportionally nor by inversely, decreasing or increasing trend. Generally, the EC (Salinity) of the Dead Sea water revealed a proportional relation with respect to the temperature changes and to the evaporation level, but the pH values decreased as the evaporation level is increased.

The simplicity of these experiments does not reproduce the sulfate contents to form Gypsum, which precipitate very advanced evaporation levels. However, in nature, the addition of Red-Dead Sea conveyance would bring rich sulfate waters to enable gypsum formation. Nevertheless, our experiments show that the major K–Mg minerals such as Bischofite, Tachyhydrite and Carnallite are formed in advanced evaporation levels. The precipitated minerals during the 12.5–20% evaporation stage can be detected by naked eye; it started to form suspended particles. The intensity of colloids increases as the evaporation levels continues. Then, the transparency decreases notably and may be considered as the starting point of “Whitening” phenomenon. The ancestor thin layer floating on the water surface is condensed and prevents, to some extent, vapor to escape from the water body. Thereafter, stalactites started to form.

**Table 7** The correlation matrix for the XRF results

	Na	Mg	K	Cl	Br	Ca	Si	P	Fe	Mn
Na	1.00									
Mg	-0.881	1.00								
K	0.13606	0.22755	1.00							
Cl	-0.66667	0.61905	0.08383	1.00						
Br	-0.69048	0.54762	0.15569	0.83333	1.00					
Ca	-0.52381	0.42857	0.05988	0.78571	0.92857	1.00				
Si	0.87427	-0.898	-0.42771	-0.51498	-0.41917	-0.28743	1.00			
P	-0.03706	0.24708	-0.64627	0.18531	0.22238	0.02471	-0.07457	1.00		
Fe	-0.35827	0.49417	-0.32314	0.40769	0.4571	0.28415	-0.51578	0.75641	1.00	
Mn	-0.17964	0.43114	-0.25904	-0.13174	-0.14372	-0.38324	-0.40964	0.71463	0.66492	1.00

**Table 8** The *P* value for the correlation coefficients presented in Table 6

	Na	Mg	K	Cl	Br	Ca	Si	P	Fe	Mn
Na	1.00	0.00385	0.13606	0.07099	0.05799	0.18272	0.00451	0.93057	0.38351	0.67034
Mg		1.00	0.58784	0.10173	0.16003	0.2894	0.00244	0.55523	0.21323	0.2862
K			1.00	0.84355	0.71276	0.88799	0.29048	0.08337	0.43497	0.5356
Cl				1.00	0.01018	0.02082	0.19155	0.66041	0.31606	0.75583
Br					1.00	0.00086	0.59659	0.59659	0.25483	0.73422
Ca						1.00	0.49002	0.95369	0.49521	0.34868
Si							1.00	0.8607	0.19074	0.31353
P								1.00	0.02985	0.04637
Fe									1.00	0.072
Mn										1.00

## References

- Arab Potash Company Annual Reports, 1993–2014
- Ben-Yaakov S, Sass E (1977) Independent estimate of the pH of Dead Sea brines. Limnol Oceanogr 22:374–376
- Beyth M (1980) Recent evolution and present stage of the Dead Sea brines. In: Nissenbaum A (ed) Hypersaline brines and evaporitic environments. Elsevier, Amsterdam, pp 155–166
- Bloch R, Littman HZ, Elazari-Volcani B (1944) Occasional whiteness of the Dead Sea. Nature 154:402–403
- Gavrieli I (1997) Halite deposition in the Dead Sea: 1960–1993. In: Niemi T, Ben-Avraham Z, Gat JR (eds) The Dead Sea—the lake and its setting. Oxford University Press, Oxford, pp 161–170
- Greenberg AE, Conners SS, Jenkins D (eds) (1980) Standard methods for the examination of water and wastewater, 15th edn. American Public Health Association, Washington
- Herut B, Gavrieli I, Halicz L (1998) Coprecipitation of trace and minor elements in modern authigenic halites from the hypersaline Dead Sea brine. Geochim Cosmochim Acta 62:1587–1598
- Margane A, Manfred H, Almomani M, Subah A (2002) Contribution to the hydrogeology of North and Central Jordan, Hannover
- Ministry of Water and Irrigation (MWI) (2013) Open Files
- Neiv D, Emery KO (1967) The Dead Sea. Depositional Processes and Environments of Evaporites. Bulletin No. 41, State of Israel, Ministry of Development, Geological Survey
- Reznik IJ, Gavrieli I, Ganor J (2009a) Kinetics of gypsum nucleation and crystal growth from Dead Sea brine. Geochim Cosmochim Acta 73:6218–6230
- Reznik IJ, Gal A, Ganor J, Gavrieli I (2009b) Gypsum saturation degrees and precipitation potential from Dead Sea–Seawater mixtures. Environ Chem 6(5):416–423
- Rice EW, Baird RB, Eaton AD (2017) Standard methods for the examination of water and wastewater, 23rd edn. American Public Health Association, American Water Works Association, Water Environment Federation, Washington
- Stein M, Starinsky A, Katz A, Goldstein SL, Machlus M, Schramm A (1997) Strontium isotopic, chemical, and sedimentological evidence for the evolution of Lake Lisan and the Dead Sea. Geochim Cosmochim Acta 61:3975–3992
- Steinhorn I, Gat JR (1983) The Dead Sea. Sci Am 249(4):102–109
- TAHAL Group (2011) Red Sea–Dead Sea Water Conveyance Study Program, Dead Sea Study, Final Report, GSI Report Number: GSI/10/2011